

tial closer to the Lang-Kohn result. The data of Levinson and Plummer¹⁶ on normal photoemission from the Al(100) Fermi level are also correctly fitted with use of this potential. Thus a steeper potential is indicated for In than for Al and this result can explain the different shape of the surface-plasmon dispersion curves of Al and In obtained by Krane and Raether.¹⁷

I would like to thank Y. Pétrouff for suggesting the experiment, stimulating discussions, and critical reading of the manuscript and Professor H. Raether for pointing out to us his work on surface-plasmon dispersion.¹⁷ I am very indebted to A. Quémerais for experimental assistance and to the technical staff of Laboratoire pour l'Utilisation du Rayonnement Electromagnétique and members of the Laboratoire de l'Accélérateur Linéaire for providing the synchrotron beam facilities.

¹S. A. Flodström and J. G. Endriz, Phys. Rev. Lett. **31**, 893 (1973).

²S. A. Flodström and J. G. Endriz, Phys. Rev. B **12**, 1252 (1975).

³J. Monin and G. A. Boutry, Phys. Rev. B **9**, 1309

(1974).

^{4a}H. Petersen and S. B. M. Hagström, Phys. Rev. Lett. **41**, 1314 (1978).

^{4b}H. Petersen, Z. Phys. B **31**, 171 (1978).

⁵P. J. Feibelman, Phys. Rev. Lett. **34**, 1092 (1975).

⁶M. L. Theye and G. Devant, Thin Solid Films **4**, 105 (1969).

⁷J. M. Elson and R. M. Ritchie, Phys. Status Solidi (b) **62**, 461 (1974).

⁸E. Leroux and M. F. Mousselly, Nouv. Rev. Opt. **7**, 57 (1976).

⁹J. Boissoles, unpublished.

¹⁰In the actual experiment, the degree of polarization of the light is 80%. However, for the sake of simplicity, I have kept the expressions *s*-polarized, *p*-polarized, *R_s*, *R_p*, Thus, *p* polarized refers to the situation where the major axis of the polarization ellipse is in the plane of incidence of light on the sample and *s* polarized to the case where the major axis is perpendicular to this plane.

¹¹These results are corrected for 80% degree of polarization.

¹²J. G. Endriz, Phys. Rev. B **7**, 3464 (1973).

¹³G. D. Mahan, Phys. Rev. B **2**, 4334 (1970).

¹⁴K. L. Kliewer, Phys. Rev. B **14**, 1412 (1976).

¹⁵J. P. Perdew and R. Monnier, Phys. Rev. B **17**, 2595 (1978).

¹⁶H. J. Levinson, E. W. Plummer, and P. J. Feibelman, Phys. Rev. Lett. **43**, 952 (1979).

¹⁷K. J. Krane and H. Raether, Phys. Rev. Lett. **37**, 1355 (1976).

Electron-Spin-Resonance and Lattice-Parameter Study of Cerium Cubic Laves-Phase Compounds: Evidence for Intermediate-Valence State

G. E. Barberis and D. Davidov

Racah Institute of Physics, Hebrew University of Jerusalem, Jerusalem, Israel, and Instituto de Física "Gleb Wataghin," Universidade Estadual de Campinas, 131000 Campinas, São Paulo, Brazil

and

C. Rettori, J. P. Donoso, I. Torriani, and F. C. G. Gandra

Instituto de Física "Gleb Wataghin," Universidade Estadual de Campinas, 131000 Campinas, São Paulo, Brazil

(Received 2 May 1980)

A lattice-constant study of the cubic $C15$ $Ce(Ir_xOs_{1-x})_2$ and $Ce(Pt_xIr_{1-x})_2$ mixtures at room temperature reveals anomalous lattice constant versus x behavior. Also the electron-spin-resonance thermal broadening and g shift of Nd^{3+} in these compounds are anomalous but could be correlated with the lattice parameters. This is taken as evidence for intermediate-valence state in some of the mixtures.

PACS numbers: 76.30.Hc, 61.55.Hg

Cerium and many of its intermetallic compounds are known to exhibit nonintegral valence.¹⁻³ The valence or the $4f$ occupation may change either continuously or discontinuously by varying the composition of the materials,^{1,4,5} external pres-

sure,¹ or temperature.^{1,6} Associated with valence change there are usually large changes in the lattice parameter and magnetic properties. Recently, concepts such as intermediate valence (IV) or interconfigurational fluctuations (ICF) have been

used to describe this very interesting state with nonintegral valence.¹

The possibility that interconfigurational fluctuations in compounds with nonintegral valence can be probed by electron-spin-resonance (ESR) measurements of Gd^{3+} has been suggested by various authors with, however, conflicting conclusions.^{7,8} Gambke, Elschner, and Hirst,⁷ based on their ESR of Gd in the ICF system $CePd_3$, have suggested that ICF state acts to reduce the Gd relaxation rate with respect to that in non-ICF system. Heinrich and Meyer,⁸ however, have observed the opposite phenomena in $CeBe_{13}:Gd$. These authors have noticed, also, a significantly large spin-flip relaxation rate for the conduction electrons in $CeBe_{13}:Gd$ which they attribute to the ICF state of $CeBe_{13}$.⁸ Certainly a critical check of these conflicting ideas requires a system in which the valence can be changed continuously. Motivated by this fact, we have carried out a lattice-constant study and ESR measurements of Nd^{3+} in the cubic C15 compounds $Ce(Ir_xOs_{1-x})_2$ and $Ce(Pt_xIr_{1-x})_2$ ($0 \leq x \leq 1$).

The elements Os, Ir, and Pt are 5d metals belonging to group VIII of the periodic table. It was hoped, therefore, that some of the physical properties and especially the valence of the Ce might be changed in a systematic manner from $CeOs_2$ via $CeIr_2$ to $CePt_2$. Indeed, $CePt_2$ is a magnetic compound ($T_c \cong 2 K$)³ and the valence of the Ce is very close to 3+; $CeOs_2$ is nonmagnetic and the Ce valence is believed to be close to 4+.³ As for $CeIr_2$, the situation is far from being clear. This compound is nonmagnetic with a Pauli paramagnetism which is only slightly larger than that of $CeOs_2$.⁹ However, recent x-ray-edge studies¹⁰ have indicated that the x-ray-edge spectra of $CeIr_2$ is very similar to that of the intermediate-valence compound $CePd_3$ but differs from the edge spectra of the quadrivalent insulator CeO_2 or $CeNi_2$. Furthermore, ESR study of Nd and Gd in $CeIr_2$ ¹¹ reveals giant thermal broadening which could not be explained by band-structure effects and may be attributed to the IV state of $CeIr_2$. Additional evidence for $CeIr_2$ being a IV compound is provided by the Ce ionic radii of various Ce cubic compounds given in the paper of Sereni, Olcese, and Rizzuto.³ It has been demonstrated³ by them that the Ce atomic radii of $CeIr_2$ is intermediate to that of $CeRu_2$ (superconducting) and $CePt_2$ (magnetic). One expects, therefore, that by mixing $CePt_2$ and $CeIr_2$ or $CeIr_2$ and $CeOs_2$ the valence can be changed in a controlled manner. Such valence changes induced by alloying have been ob-

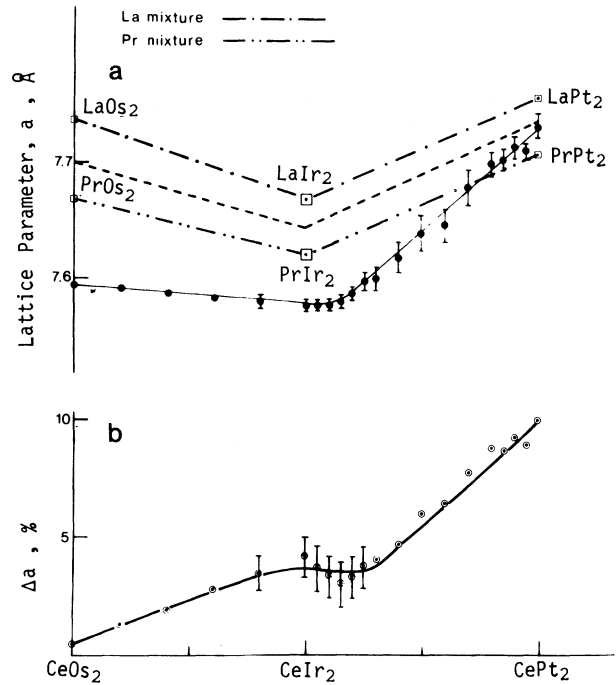


FIG. 1. (a) Lattice parameter, a , of the mixtures $Ce(Ir_xOs_{1-x})_2$ and $Ce(Pt_xIr_{1-x})_2$ (closed circles) at room temperature. The solid line connecting the data points in (a) is a guide to the eye. For comparison the lattice constants of the analogous La and Pr mixtures are shown by the dashed-dotted lines in the same figure. The lattice parameters of LaX_2 and PrX_2 ($X = Os, Ir, Pt$) were taken from Compton and Matthias (Ref. 12). (b) The percentage variation of the lattice parameter associated with the variation of the Ce ionic radius as extracted by subtracting the dashed line from the solid line in Fig. 1(a) (see text). The solid line in (b) is a guide to the eye.

served recently in the systems $CeRh_{3-x}Pd_x$ ⁵ and $UNi_{5-x}Cu_x$.⁴ If this is indeed the case, then the systems $Ce(Ir_xOs_{1-x})_2$ and $Ce(Pt_xIr_{1-x})_2$ doped with Nd^{3+} impurities might be ideal for checking the above-mentioned ideas concerning the ESR of ICF systems.

We shall discuss, firstly, the lattice-constant measurements. These were carried out either by x-ray diffractometer method or by the Debye-Scherrer method at room temperature without any differences between the two methods. Figure 1(a) exhibits the lattice parameters of the systems $Ce(Ir_xOs_{1-x})_2$ and $Ce(Pt_xIr_{1-x})_2$. It indicates that the lattice constant changes continuously, slightly decreasing with x for $Ce(Ir_xOs_{1-x})_2$ ($0 \leq x \leq 1$), almost constant for $Ce(Pt_xIr_{1-x})_2$ in the range $0 \leq x \leq 0.15$, and increases significantly towards $CePt_2$

in the range $0.15 < x \leq 1$. The lattice constant of the system $\text{Ce}(\text{Pt}_x\text{Ir}_{1-x})_2$ is certainly anomalous and reflects, in our best judgment, a change in the Ce valence. To estimate the variation of the lattice constant due to the change of the Ce valence, a comparison with the lattice parameters of the trivalent La and Pr analogous compounds is very desirable. In Fig. 1(a) we have plotted the lattice parameters of the analogous Pr and La compounds (see dashed-dotted lines). These dashed-dotted lines were obtained by using the published data of Compton and Matthias¹² as well as Vegard's law. It should be noted that the lattice constants of CeOs_2 , CeIr_2 , and CePt_2 measured in the present work are also consistent with those measured by Compton and Matthias.¹² As clearly seen in Fig. 1(a), the lattice parameter of CePt_2 falls exactly between those of LaPt_2 and PrPt_2 indicating that indeed Ce in CePt_2 exhibits a valence close to 3+. Other supporting evidence for this conclusion is provided by lattice-parameter calculation using a closed-packet model for CePt_2 and the atomic radius of Ce^{3+} from the table of Sergent-Welch.¹³ This calculation yields $a_0(\text{CePt}_2) = 7.71 \text{ \AA}$, very close to the experimental lattice parameter. The rest of the Laves-phase mixtures of cerium exhibit significantly smaller lattice parameter with respect to those expected theoretically if we assume that Ce has 3+ valence in all the mixtures [see dashed line in Fig. 1(a)]. This deviation is attributed to valence change as well as to band-structure effects. The latter effect can be verified from the concentration dependence of a in the La and Pr mixtures [dashed-dotted lines in Fig. 1(a)]. Thus, by subtracting the concentration dependence of the lattice constant of the Pr and La mixtures from our experimental data for the Ce mixtures, one can find the change in the lattice parameter, Δa , associated with the change in the Ce ionic radius. The value of Δa extracted by this procedure is exhibited in Fig. 1(b). As clearly seen, Δa increases from CeOs_2 to CePt_2 by 10% approximately but exhibits some anomaly in the vicinity of CeIr_2 . It should be mentioned that a change in the lattice constant of the same order of magnitude (11%) has been observed in Ce metal corresponding to a valence change from the magnetic (γ phase) to the nonmagnetic (α' phase).^{2,6} If one assumes that a 11% change in the lattice constant corresponds to a change of the Ce atomic radius from that appropriate to 4+ valence to that of 3+, then one can estimate the valence of CeOs_2 to be 3.90 by using a simple linear interpolation method.

The increase of Δa [Fig. 1(b)] from CeOs_2 to CeIr_2 strongly supports the existence of intermediate-valence state for this last compound, although this last feature does not reflect itself in the measured susceptibility.⁹

We turn now to discuss our ESR results. We have used both Nd^{3+} and Gd^{3+} as probe ions in the various intermetallic mixtures. However, the Gd^{3+} resonance yields large residual width, which makes the analysis difficult. In the following, we shall concentrate mainly on the Nd^{3+} ESR properties. The Nd^{3+} ion with angular momentum $J = \frac{9}{2}$ splits in the cubic crystalline field into one Γ_6 doublet and two Γ_8 quarters. Our measurements indicate that the Γ_6 is the ground state in most of our hosts except, maybe, for $\text{Ce}(\text{Pt}_x\text{Ir}_{1-x})_2$ in the concentration range $0.85 < x \leq 1$ where no Nd^{3+} resonance associated with Γ_6 ground state could be detected (but Er and Yb resonances with Γ_7 ground state could be observed). The inset of Fig. 2 yields ESR spectra of $\text{CeOs}_2:\text{Nd}$ with naturally abundant Nd, as an example. As seen, the central line corresponding to ^{144}Nd isotope is surrounded by many hyperfine satellites appropriate to the ^{143}Nd and ^{145}Nd isotopes. These satellites yield hyperfine constants of $A(^{143}\text{Nd}) = 204.4 \text{ G}$ and $A(^{145}\text{Nd}) = 126.3 \text{ G}$. To the best of our knowledge the hyperfine spectra in the inset of Fig. 2 represent the best-resolved spectra ever observed in ESR in metals.

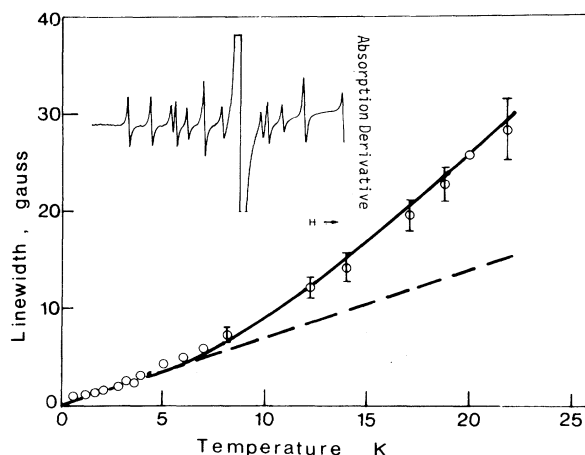


FIG. 2. The ESR linewidth of the central line (after subtracting the residual width) of $\text{CeOs}_2:\text{Nd}$ (400 ppm; natural abundance). The solid line is a theoretical fit to the theory of Hirst (Ref. 14). This fit yields a splitting 112 K between the Γ_6 ground state and the Γ_8 first excited state. The dashed line represents the Korringa thermal broadening. The inset represents the spectra of $\text{CeOs}_2:\text{Nd}$ at $T = 1.5 \text{ K}$.

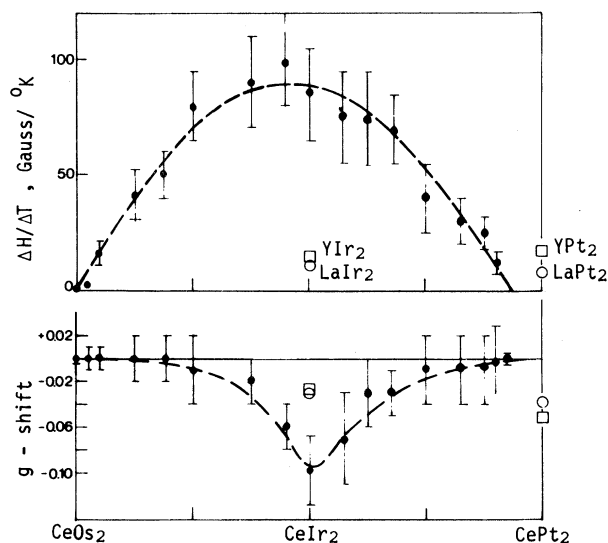


FIG. 3. The initial thermal broadening, $\Delta H/\Delta T$, and the ESR g shift for the various $\text{Ce}(\text{Ir}_x\text{Os}_{1-x})_2\text{:Nd}$ and $\text{Ce}(\text{Pt}_x\text{Ir}_{1-x})_2\text{:Nd}$ mixtures. The dashed lines are guides to the eye. For comparison, the ESR thermal broadening and g shifts of Nd in the analogous YX_2 and LaX_2 compounds ($\text{X} = \text{Ir}, \text{Pt}$) are also given.

The ESR linewidth of the central line as a function of temperature is given in Fig. 2. The ESR thermal broadening exhibits linear behavior at low temperatures but shows a deviation from linearity for $T > 7$ K. This deviation is attributed to the presence of a Γ_8 excited state at energy splitting $\Delta = 112$ K according to the model of Hirst.¹⁴ The initial thermal broadening $\Delta H/\Delta T$ is 0.7 G/K for CeOs_2 . The data for the rest of the compounds was analyzed in the same way. In Fig. 3, we have plotted the initial thermal broadening $\Delta H/\Delta T$ as well as the Nd^{3+} g shift (measured with respect to $g = 2.667$ appropriate to $\text{Nd}^{3+} \Gamma_6$ g value in insulators) for the various $\text{Ce}(\text{Ir}_x\text{Os}_{1-x})_2$ and $\text{Ce}(\text{Pt}_x\text{Ir}_{1-x})_2$ systems. A striking feature of our results in Fig. 3 is the dramatic variation of the ESR thermal broadening and g shift by at least two orders of magnitude (note that $\Delta H/\Delta T \cong 100$ G/K for CeIr_2 but it is only 0.7 G/K for CeOs_2). This dramatic variation *cannot* be explained by band-structure effects or by the variation of the host susceptibility. Recent ESR study of Gd and Nd in the non-ICF hosts Y and La compounds have shown only slight variation in the ESR thermal broadening across the series¹¹ (see for example, the values of $\Delta H/\Delta T$ and Δg for Nd^{3+} in LaIr_2 , YIr_2 , LaPt_2 , and YPt_2 in Fig. 3). The Gd g shift across the analogous hosts, however, was

found to change from negative value in $\text{LaOs}_2\text{:Gd}$ to positive value in $\text{LaPt}_2\text{:Gd}$ being very small in $\text{LaIr}_2\text{:Gd}$. This last feature could be explained very well by band-structure effects.¹¹ Clearly, the situation in the Ce analogous series is different and our results in Fig. 3 call for a different mechanism. The possible existence of intermediate valence in some of our compounds provides some realistic mechanism to explain the ESR features.

A very attractive model that is frequently used to describe intermediate-valence systems and can be used also to describe qualitatively the ESR features in Fig. 3 is the virtual-bound-state (VBS) model. (See the review paper of Robinson, Ref. 1). In this model, the $4f$ level is broadened by covalent admixture with the conduction electrons to form $4f$ virtual bound state with $4f$ density of states given by $n_f(E) = (\Delta/\pi)[(E - E_F)^2 + \Delta^2]^{-1}$. Here Δ is the VBS width and E_F is the Fermi energy. The ESR properties ($\Delta H/\Delta T$ and Δg) depend on the density of Ce $4f$ electrons at the Fermi level, $n_f(E_F)$, as well as on the densities of s and d electrons, according to a modified Korringa mechanism. Thus, for magnetic Ce (valence $3+$ as in CePt_2), the $4f^1$ level with up spin lies below the Fermi level with a very small overlap $n_f(E_F)$ with the Fermi level. In this case no contribution to the ESR properties associated with the Ce $4f$ electrons is expected. The decrease of the lattice constant shifts the Fermi level and is accompanied by a decrease of $E_{4f} - E_F$. In the limit $\Delta \gg E_{4f} - E_F$, $n_f(E_F) = 1/\pi\Delta$ and the virtual $4f$ state overlaps with the Fermi level. In this case additional contributions to the ESR properties are expected because of large density of Ce $4f$ states at the Fermi level. Simple arguments⁹ indicate that this additional contribution to $\Delta H/\Delta T$ and Δg is proportional to $(J/\Delta)^2$ and J/Δ , respectively; here J is the coupling constant between the Nd^{3+} and the fluctuating bath. This contribution might be much larger than the usual Korringa mechanism due to s, d electrons. This might be the case appropriate to $\text{Ce}(\text{Pt}_x\text{Ir}_{1-x})_2$ $0 \leq x \leq 0.15$. Further decrease of the lattice constant shifts the $4f$ level above the Fermi level, resulting in a significant reduction of $n_f(E_F)$. This might be the $\text{CeOs}_2\text{:Nd}$ case. It should be mentioned, at this stage, that while the susceptibility of the system $\text{Ce}(\text{Pt}_x\text{Ir}_{1-x})_2$ generally increases with x ,⁹ the ESR properties (Fig. 3) decrease with x . This indicates that the ESR properties do not reflect the total host susceptibility but rather the density of f (and s, d) electrons at the Fermi

level. It should be stressed, also, that the susceptibility of the system $\text{Ce}(\text{Ir}_x\text{Os}_{1-x})_2$ is relatively small which is not very "typical to ICF systems" and somewhat inconsistent with our VBS picture.

In summary, the lattice-constant study indicates that mixtures in the vicinity of CeIr_2 exhibit intermediate-valence state of the cerium (Fig. 1). On the assumption that the Ce $4f$ state can be described by a VBS model, the ESR properties support the idea of intermediate-valence state. Preliminary susceptibility study⁹ is not completely consistent with this interpretation. This might indicate that our VBS picture is somewhat naive and that further experiments like x-ray-photoemission spectroscopy as well as theory are needed. Our work clearly indicates, however, that the narrowing mechanism of Gambke, Elschner, and Hirst⁷ is not typical to ICF systems.

Useful discussions with Professor L. Falicov, Professor D. K. Wollleben, and Dr. I. Felner are acknowledged with thanks. This work was supported in part by the Fundação de Amparo à Pesquisa do Estado de São Paulo, and by the Conselho Nacional 170 de Desenvolvimento Científico e Tecnológico, Brazil.

¹D. K. Wollleben, *J. Phys. (Paris), Colloq.* **40**, C4-233 (1979); J. M. Robinson, *Phys. Rep.* **51**, 1 (1979).

²R. Ramiraz and L. M. Falicov, *Phys. Rev. B* **3**, 2425 (1971).

³J. G. Sereni, G. L. Olcese, and C. Rizzuto, *J. Phys. (Paris), Colloq.* **40**, C5-337 (1979).

⁴H. J. Van-Daal, K. H. J. Buschow, P. B. Van Aken, and M. H. Von Maaren, *Phys. Rev. Lett.* **34**, 1457 (1975).

⁵I. R. Harris, M. Norman, and W. E. Gardner, *J. Less Common Met.* **21**, 277 (1972).

⁶S. M. Shapiro, J. D. Axe, R. J. Birgeneau, J. M. Lawrence, and R. D. Parks, *Phys. Rev. B* **16**, 2225 (1977).

⁷T. Gambke, B. Elschner, and L. L. Hirst, *Phys. Rev. Lett.* **40**, 1290 (1978).

⁸G. Heinrich and A. Meyer, *Solid State Commun.* **24**, 1 (1977).

⁹G. E. Barberis and D. Davidov, to be published.

¹⁰H. Launois, M. Rawiso, R. Pott, E. Holland-Moritz, J. Sereni, R. Boksich, and D. Wollleben, to be published.

¹¹G. E. Barberis, D. Davidov, J. P. Donoso, C. Rettori, J. F. Suassuna, and H. D. Dokter, *Phys. Rev. B* **19**, 5495 (1979).

¹²V. B. Compton and B. T. Matthias, *Acta Crystallogr.* **12**, 651 (1959).

¹³*Periodic Table of the Atoms* (Sergent-Welch, Skokie, Illinois, 1969).

¹⁴L. L. Hirst, *Phys. Rev.* **181**, 597 (1969).

Evidence for Bose-Einstein Statistics in an Exciton Gas

D. Hulin, A. Mysyrowicz, and C. Benoît à la Guillaume

*Groupe de Physique des Solides de l'École Normale Supérieure, Université Paris VII,
Place Jussieu, F-75221 Paris 05, France*

(Received 9 April 1980)

A free-exciton gas is studied as a function of generated particle density in Cu_2O at 1.5 K. A line-shape analysis of the subsequent recombination shows a gradual evolution, from a classical regime at low density, to a highly quantum-statistical one with chemical potential $\mu \approx 0$.

PACS numbers: 76.30.Hc, 61.55.Hg

It is well known that in an ideal Bose gas the energy distribution of the particles obeys the relation

$$N(E) = \rho(E)f(E), \quad (1)$$

where $\rho(E) = AE^{1/2}$ is the density of states, $f(E) = \{\exp[(E - \mu)/KT] - 1\}^{-1}$ is the occupation number of levels of energy E , measured from the lowest level $E = 0$, and μ is the chemical potential of the gas, determined by the condition that $\sum_E N(E) = N_t$, the total number of particles. In usual situations, the ratio $-\mu/KT \gg 1$ and relation (1) is very well approximated by Maxwell-Boltzmann distribution. If $-\mu/KT < 2$, differences from classical statistics

occur, with a tendency for the particles to accumulate in the states of lowest energy. This quantum attraction effect becomes precipitous if $N_t > N_c = 6.2 \times 10^{15} g(m/m_0)^{3/2} T^{3/2}$ (m_0 , free-electron mass; m particle mass; g , degeneracy factor), for which $\mu = 0$, giving rise to a phase transition with a macroscopic occupation of a single quantum state $E = 0$ [Bose-Einstein condensation (BEC)]. It is generally admitted that BEC is the physical origin of the spectacular properties of ^4He below the λ point although an interpretation using the ideal Bose gas as a starting point raises serious questions, because of the strong interactions between atoms in liquid helium. It is therefore im-